



Polímeros: Ciência e Tecnologia

ISSN: 0104-1428

abpol@abpol.org.br

Associação Brasileira de Polímeros  
Brasil

Rodrigues, Arieny; Carvalho, Benjamim de M.; Pinheiro, Luís A.; Bretãs, Rosário E. S.; Canevarolo, Sebastião V.; Marini, Juliano

Effect of Compatibilization and Reprocessing on the Isothermal Crystallization Kinetics of Polypropylene/Wood Flour Composites

Polímeros: Ciência e Tecnologia, vol. 23, núm. 3, julio-septiembre, 2013, pp. 312-319

Associação Brasileira de Polímeros  
São Paulo, Brasil

Disponível em: <http://www.redalyc.org/articulo.oa?id=47027957018>

- Como citar el artículo
- Número completo
- Más información del artículo
- Página de la revista en redalyc.org

redalyc.org

Sistema de Información Científica

Red de Revistas Científicas de América Latina, el Caribe, España y Portugal

Proyecto académico sin fines de lucro, desarrollado bajo la iniciativa de acceso abierto

# Effect of Compatibilization and Reprocessing on the Isothermal Crystallization Kinetics of Polypropylene/Wood Flour Composites

Arieny Rodrigues, Benjamim de M. Carvalho, Luís A. Pinheiro  
*State University of Ponta Grossa, UEPG*

Rosário E. S. Bretãs, Sebastião V. Canevarolo, Juliano Marini  
*Department of Materials Engineering, UFSCar*

**Abstract:** Numerous studies have focused on polymer mixtures aimed at the potential applications of these materials. This work analyzed the effect of polymer reprocessing and the type and concentration of compatibilizer on the isothermal crystallization kinetics of polypropylene/wood flour composites. The composites, which were polypropylene grafted with acrylic acid (PP-g-AA) and maleic anhydride (PP-g-MA), were processed in a twin screw extruder with and without compatibilizer. Reprocessed polypropylene reached complete crystallization in less time than the composites with virgin polypropylene. The addition of wood flour to the composites did not change the kinetics significantly compared to that of the pure polymers, but the compatibilizers did, particularly PP-g-AA. The nucleation exponent ( $n$ ) and crystallization rate ( $K$ ) were calculated from Avrami plots. The values of  $n$  ranged from 2 to 3, indicating instantaneous to sporadic nucleation. The crystallization half-time of reprocessed polypropylene was shorter than that of virgin polypropylene and of the compositions containing PP-g-AA compatibilizer. The activation energy of crystallization and the equilibrium melting temperature were calculated, respectively, from Arrhenius and Hoffman-Weeks plots. Both of these parameters showed lower values in the composites, particularly in the ones containing compatibilizers.

**Keywords:** *Polypropylene, reprocessing, wood flour, composites, compatibilizers, isothermal crystallization.*

## Introduction

Several technologies involving the use of recycled plastic-wood composites as an alternative to natural wood profiles, mainly for the manufacture of decking and fencing, emerged in the USA in the 1990s. These materials were dubbed recycled plastic lumber (RPL). Later, this type of material was given the generic term 'wood plastic composite' (WPC)<sup>[1,2]</sup>.

The use of cellulose reinforcement fibers in thermoplastic composites has been studied extensively<sup>[3-6]</sup>, because they optimize the properties of these composites. Wood fibers are reported in the literature as the main factor for improvement of properties such as elasticity modulus<sup>[7]</sup>. These composites can be produced according to several processing methods, but perhaps the most interesting one is extrusion, particularly twin screw extrusion, whose mixing capacity enables better secondary phase dispersion. This extruder also requires a short residence time, which is an important aspect because it is sufficiently brief to avoid degradation but long enough for all the compatibility reactions to take place<sup>[8-11]</sup>.

To ensure the satisfactory mechanical performance of WPC it is required the integrity of the polymer-wood interface. In some situations, this can only be achieved with compatibilizers<sup>[4]</sup>, which react with both phases and strongly bind them together. This bond is the key factor for good stress transfer from polymer to filler, enhancing

the composite's mechanical strength. The presence of compatibilizer at the polymer/filler interface decreases the interfacial tension between wood and polymer, increasing the adhesion between them, and also provides wettability, thus preventing agglomeration. According to the literature, the compatibilizer most commonly used is maleic anhydride, which is usually grafted onto a polymer matrix<sup>[12]</sup>.

Crystallization is a crucial step in polymer processing because it determines the material's crystalline morphology. During cooling, the presence of reinforcing filler in the polymer matrix can modify the formation of crystals in the composite when compared with pure polymer. This fact has motivated numerous studies about crystallization kinetics, which have shown that reinforcing fillers modify the optical and mechanical properties of these materials<sup>[13-15]</sup>. Like all transitions, crystallization obeys specific thermodynamic conditions in which the crystal may or may not exist and which are determined by the kinetics of the process. Many studies about crystallization kinetics have used the Avrami equation<sup>[16-21]</sup>. Although it applies to isothermal conditions that are not usually observed in processing methodologies, Avrami treatment is useful for inferring important parameters, such as the kind of crystallized structure and nucleation of the crystallization process.

The work reported here involved an evaluation of the crystallization kinetics of polypropylene/wood flour composites compatibilized with maleic anhydride (PP-g-MA) and acrylic acid (PP-g-AA). The use of reprocessed PP in the above described conditions was also analyzed to evaluate the influence of recycled polymer on the crystallization of the composites.

## Experimental

### Materials

Wood flour (100 mesh) supplied by Pinhopó Ltda, Ponta Grossa, Brazil was mixed with H301 polypropylene (MFI = 10 g/10 min) donated by Braskem S.A. The compatibilizers were Polybond 1001, a polypropylene-acrylic acid copolymer (PP-g-AA), and Polybond 3200, a polypropylene-maleic anhydride copolymer (MFI = 40 and 100 g/10 min, respectively), both from Chemtura Brasil. The functional groups concentrations of acrylic acid and maleic anhydride were determined by titration<sup>[22]</sup> and they were found equal to 605 and 578 µg/g, respectively.

### Preparation of the composites

The polypropylene-wood flour composites were prepared in a ZSK-30 twin screw extruder (Werner & Pfleiderer). The wood content was kept constant at 10% (w/w). The concentrations of compatibilizer used were 5 and 10% (w/w), considering the total composite weight. The remaining fraction was completed with H301 polypropylene. The wood flour was previously dried at 60 °C for 24 hours. All the compositions were reproduced using reprocessed polypropylene, which consisted of the same H301 polypropylene extruded once and then ground and mixed with wood flour and compatibilizer.

The screw profile for the preparation of the composites is shown in Figure 1. The extrusion screw had L/D ratio of 33.5 and was assembled with a melt seal at the end of the first third of this length in order to ensure the complete melting of the polymer. The wood flour was fed into the

extruder through a side feeder at the end of the second third of the screw length to ensure a sufficiently short residence time to prevent degradation. A set of kneading discs was also mounted at this point to provide good dispersive and distributive mixing, ensuring the breakup of agglomerates and the homogeneity of the composite. The feeding system consisted of three gravimetric feeders, one for each material. The extruder temperature in the five heating zones and the die was set at 220 °C. The extruder operated at a screw speed of 100 rpm, and a feed rate of 10 kg/h.

In this paper, the compositions containing virgin and reprocessed polypropylene are identified as vPP and rPP, respectively.

### Rheological tests

Rheological tests were carried out to evaluate the degree of degradation. These tests were performed in a parallel plate Ares rheometer with controlled deformation (Rheometric Scientific Inc.). The shear modulus ( $G'$  and  $G''$ ) vs. frequency ( $\omega$ ) was plotted in the frequency range of 0.1 to 100 rad/s. The tests were performed at 190 °C in a nitrogen atmosphere and the samples were used as pellets.

### Crystallization tests

Crystallization was examined in a Shimadzu DSC-60 differential scanning calorimeter. The samples for these tests were hot-pressed for 90 s at 180 °C into thin films, chopped into square flat pieces weighing approximately 5.0 mg, and placed in an aluminum pan. The purpose of this procedure was to ensure the contact of all the material with the surface of the pan, thus avoiding problems of heat transfer from the calorimeter to the samples.

Non isothermal experiments took place in order to verify the beginning of crystallization process with cooling rate. Samples were heated up to 200 °C and cooled at 20, 15, 10, and 5 °C/min until 50 °C.

In isothermal tests, each sample was heated to 200 °C for 5 minutes at 10 °C/min. After 3 min, the temperature was reduced at 50 °C/min to the isothermal temperature

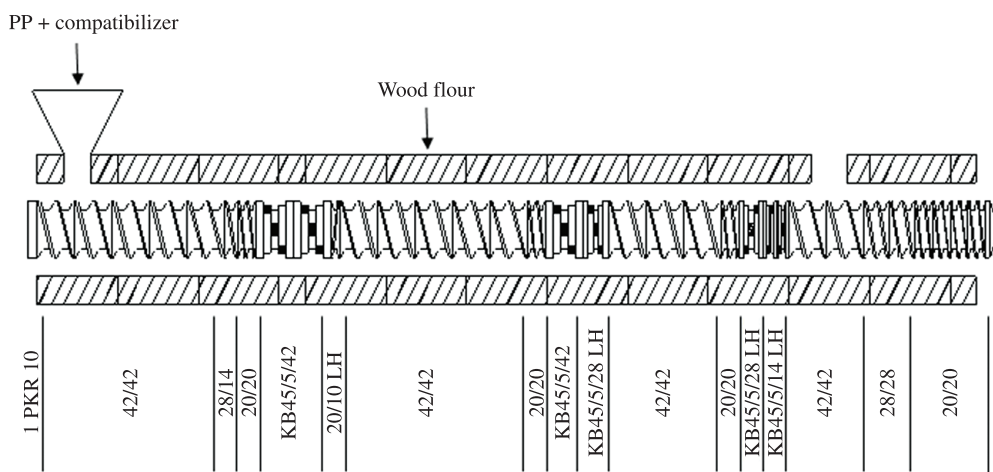


Figure 1. Screw profile used for composites obtainment.

and held there for a sufficient period of time to complete isothermal crystallization, which took place at 127, 129, 132, and 134 °C. After crystallization, the samples were reheated to 200 °C at 10 °C/ min for 5 min and the melting transition temperature was recorded. All the tests were performed under nitrogen flow of 50 mL/ min.

## Results and Discussion

### Rheological behavior

When plotted against frequency ( $\omega$ ), the curves of storage ( $G'$ ) and loss module ( $G''$ ) produces an intersection point, which changes according to the variation in polymer structure. The displacement of this point occurs at higher values of  $\omega$  with lower molecular weights (MW) and at higher values of modulus with narrow molecular

weight distributions (MWD)<sup>[23]</sup>, revealing a trend in the molecular weight distribution curve. Figure 2 shows this plot for vPP and rPP. The intersection point of rPP was shifted to higher values of  $\omega$  and  $G$  in relation to vPP. This behavior is ascribed, respectively, to decreasing molecular weight and narrowing of the MWD curve<sup>[24-26]</sup>. Because the rPP had already been processed once, it showed higher degradation than the vPP. This is consistent with the literature, which states that polypropylene undergoes chain scission during processing, especially high molecular weight polypropylene.

### Isothermal crystallization kinetics

The isothermal crystallization peaks at each temperature for each material were integrated to draw a curve of the relative crystallinity ( $X(t)$ ) as function of time. Figure 3 shows the progress of crystallization results

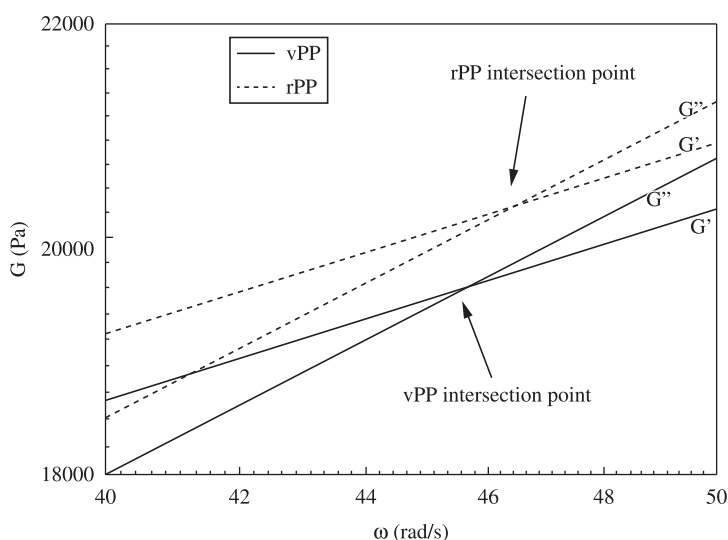


Figure 2. Modulus plot vs. frequency for vPP and rPP. The arrows mark the intersection point of each material between the  $G'$  and  $G''$  lines.

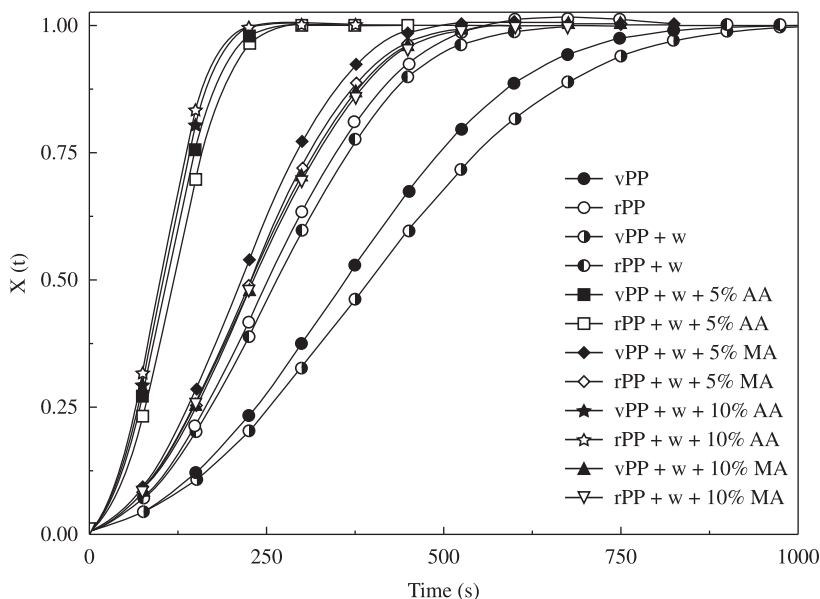


Figure 3. Progress of crystallization process over time for isotherm at 132 °C. The abbreviation 'w' is for wood.

for virgin (vPP) and reprocessed polypropylene (rPP) composites obtained at 132 °C. The results obtained at the other temperatures are not shown, since they followed the same trend.

Note the significant difference in vPP and rPP crystallization kinetics, i.e., rPP crystallizes much more rapidly than vPP. As stated on Figure 2 reprocessed PP was more degraded than virgin PP because it had already undergone one extrusion. During degradation, polypropylene undergoes chain scission, which reduces its molecular weight. Besides, literature reports an increase in oxidation degree in polymeric chains<sup>[27]</sup>, which leads to a slight increase on macromolecular polarity. For the same supercooling, the decrease in molecular weight gives rise to increase the spherulitic growth rate; on the other hand, the rate of nucleation is increased with the increase in polarity<sup>[27]</sup>. Both factors contribute to increase the overall crystallization rate, as observed on Figure 3. Considering Avrami treatment for isothermal experiments the count of time in crystallization fraction starts with the beginning of the crystallization, and it is not possible to infer whether nucleation or growth mechanisms that changes. In order to verify this effect, non isothermal experiments took place and the crystallization temperature onset ( $T_{ic}$ ) was taken versus cooling rate as shown in Figure 4. As expected, there is a general behavior of decreasing  $T_{ic}$  as cooling rate increases. The  $T_{ic}$  for vPP is lower than rPP for all cooling rates, meaning that the nucleation for the latter takes place first, due to the increase in polarity as mentioned before<sup>[27]</sup>. The results of non isothermal crystallization will not be deepened because they will be issue of further articles.

The addition of wood flour to either virgin or reprocessed PP leads to an increase in  $T_{ic}$ , showing the wood's nucleation effect on polypropylene. However, the time for entire crystallization (Figure 3) for compositions with wood is higher than that for pure polymers, which can be attributed to the slower growth stage. In this sense, wood acts as nucleating, but disturbs the crystals growth due to physical barrier. This behavior was observed by Somnuk et al.<sup>[28]</sup>, studying quiescent crystallization of polypropylene and its composites with natural fibers (vetiver grass and rossells). They found that the growth rate for neat PP in the bulk was noticeably higher than those of natural fibers composites. According to the author this may be attributed to the restriction of natural fibers on crystallization process. However, in the present work the growth rate was not measured, being an issue for further works.

The use of PP-g-AA to compatibilize wood flour with both types of PP caused  $T_{ic}$  to increase and the crystallization curves to shift toward shorter times. The effect of PP-g-AA as an efficient nucleating agent is well reported in the literature<sup>[17]</sup>. The crystallization process is slightly sensitive to the concentration of the compatibilizer and it is observed that the higher concentration in both vPP and rPP hastened the crystallization process. The compatibilizer PP-g-MA increased  $T_{ic}$  when virgin PP was used showing nucleating effect, and accelerated the overall crystallization process in comparison with vPP. When PP-g-MA was used with wood and reprocessed PP

it was observed lower  $T_{ic}$  values than pure rPP, but the overall crystallization took place faster. The concentration of PP-g-MA did not cause a significant change in the crystallization process but, unlike PP-g-AA, the lowest concentration hastened the process.

### Determination of Avrami's parameters

The relative crystallinity,  $X(t)$ , is a function of crystallization time, according to Avrami's equation:

$$X(t) = 1 - \exp(-K \cdot t^n) \quad (1)$$

where  $n$  is the Avrami exponent that is a function of type of nucleation and crystal geometry, and  $K$  is the constant rate of isothermal crystallization which depends upon nucleation and growth rate. Figure 5 shows an  $\ln[-\ln(1-X(t))]$  x  $\ln t$  plot for vPP and rPP at all the tested crystallization temperatures ( $T_c$ ). For Avrami's plot, the regression coefficients ( $r^2$ ) achieved was higher than 0.999 for all samples.

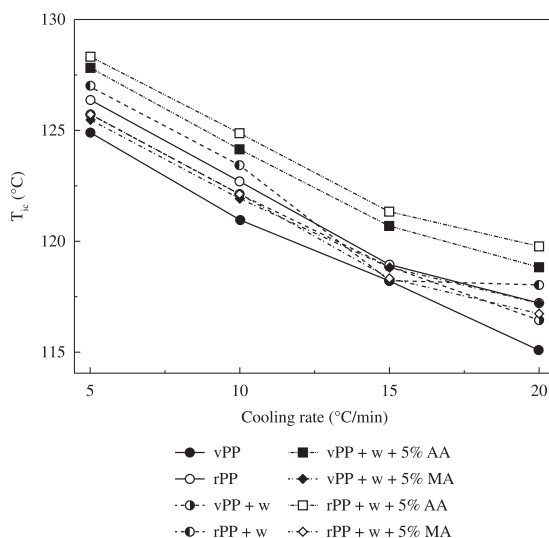


**Figure 4.** Crystallization temperature onset as function of crystallization rate. The abbreviation 'w' is for wood.

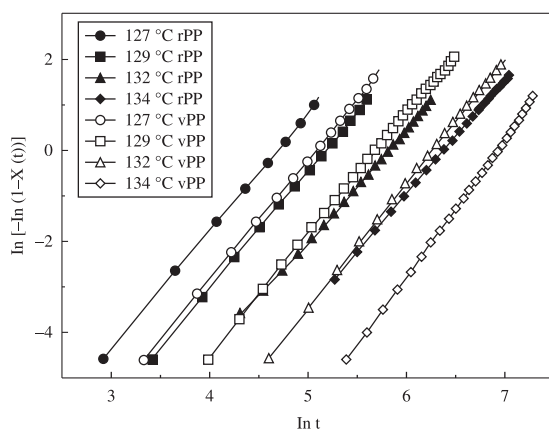


**Figure 5.** Avrami curves for virgin and reprocessed polypropylene. The hollow symbols indicate vPP while the solid symbols represent rPP.



Avrami plots were drawn only for vPP and rPP, but the other compositions follow the same trend. The plots of all the samples covered the relative crystallinity range from 0.1 to 100%. As can be seen, the curves are perfectly straight, with a single slope, indicating that primary crystallization prevailed. Zhang et al.<sup>[29]</sup> studied the crystallization kinetics of UHMWPE in liquid paraffin and created an  $\ln[-\ln(1-X(t))]$  x  $\ln t$  plot with different slopes, which they attributed to primary and secondary crystallization. In some conditions, secondary crystallization is significant and occurs in the final stages of crystallization. However, in this work, secondary crystallization was negligible or absent, as the curves in Figure 5 demonstrate. At all the crystallization temperatures, the rPP curves showed shorter times than the vPP curves at the same  $T_c$ .

The plot in Figure 5 also shows the regression-calculated values of  $n$  and  $K$ , where the former is the slope of the curve and the latter the intercept with the y-axis, all of which are listed in Table 1. These values were not calculated for the compositions with 5 and 10% of PP-g-AA at 127 °C because the curve could not be obtained due to the faster crystallization.

The literature reports that  $n$  equals 2, 3, and 4, indicating one, two and three dimensions of growth, respectively. Under quiescent conditions, the morphology of crystallized polymers shows mainly spherulitic structure resulting from the nucleation of three-dimensional crystals growing radially in every direction, with an  $n$  value of 3 for instantaneous nucleation<sup>[16,17]</sup>. In our study, most of the  $n$  values were nonintegral in the range of 1.9 to 2.3. The same order of values was observed by Kim, Harper and Taylor<sup>[18]</sup>. As observed in Figure 4, wood and compatibilizers have nucleation effect, denoting that it is difficult a transition from instantaneous to sporadic nucleation. Thus, this difference can be attributed probably to changes on crystals geometry, from three dimensions spherulites to crystals with lower dimensions. However, it is common to observe in literature values of  $n$  that can not be associated with crystals geometry<sup>[16,30]</sup>, and the differences observed for its values are due to secondary crystallization and the intricate forms of nucleation. Quillen et al.<sup>[31]</sup>

demonstrated that the presence of a transcrystalline layer changes the  $n$  value obtained through Avrami analysis. In our study, this change stemmed from variations in the shapes of crystals due to alterations in the nucleation process resulting from the inclusion of wood flour, filler that acts as a heterogeneous nucleating agent of PP. Kim, Harper and Taylor<sup>[18]</sup> also attributed the  $n$  values observed to the increase in nucleation density due to the presence of wood, which changes the shape of crystals comparing with neat PP. There are no significant variations in  $n$  values, according to Table 1, showing that this parameter is not influenced by crystallization temperature, presence of wood, type and concentration of compatibilizer.

The crystallization half-time ( $t_{1/2}$ ), i.e., the point at which relative crystallinity reaches 50%, and the isothermal crystallization rate constant,  $K$ , is inversely proportional to it. The values of  $t_{1/2}$  showed in Figure 6 were directly taken from progress of crystallization plots as draw in Figure 3, but a comparison with calculated

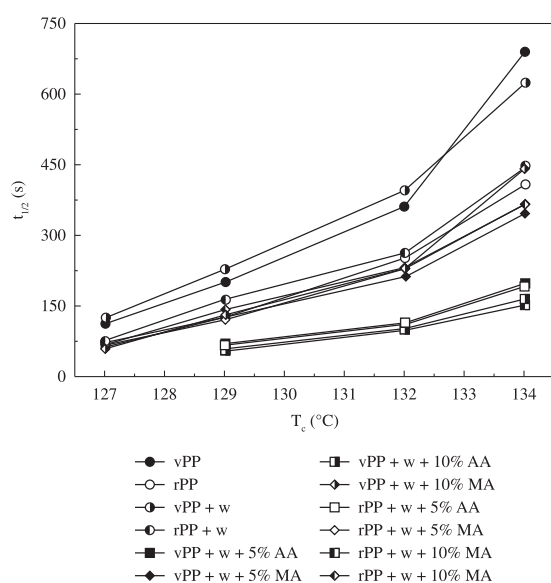


**Figure 6.** Plot of  $t_{1/2}$  with  $T_c$  for the isothermal crystallization of vPP and rPP and their respective wood flour composites. The abbreviation 'w' is for wood.

**Table 1.** Avrami parameters of isothermal crystallization.

Sample	127 °C		129 °C		132 °C		134 °C	
	n	K	n	K	n	K	N	K
vPP	2.2	2.4E-05	2.1	10.0E-06	2.2	2.2E-06	2.3	2.7E-07
vPP + wood	2.1	3.4E-05	2.0	1.1E-05	2.1	2.6E-06	2.1	8.9E-07
5% PP-g-AA	-	-	2.2	7.4E-05	2.2	2.2E-05	2.2	5.8E-06
5% PP-g-AM	2.1	1.3E-04	2.1	3.3E-05	2.2	6.6E-06	2.0	7.4E-06
10% PP-g-AA	-	-	2.2	9.0E-05	2.2	2.6E-05	2.3	5.7E-06
10% PP-g-AM	2.1	1.5E-04	2.0	4.0E-05	2.2	5.2E-06	2.0	3.0E-06
rPP	1.9	1.6E-04	2.0	5.1E-05	2.1	5.9E-06	2.0	3.6E-06
rPP + wood	2.0	1.2E-04	2.1	1.4E-05	2.1	4.9E-06	2.1	1.8E-06
5% PP-g-AA	-	-	2.2	6.8E-05	2.2	2.0E-05	2.2	6.0E-06
5% PP-g-AM	2.1	1.1E-04	2.1	3.2E-05	2.2	4.5E-06	2.1	3.5E-06
10% PP-g-AA	-	-	2.2	1.2E-04	2.2	3.0E-05	2.2	1.3E-05
10% PP-g-AM	2.0	1.7E-04	2.1	2.2E-05	2.1	7.4E-06	2.0	4.6E-06

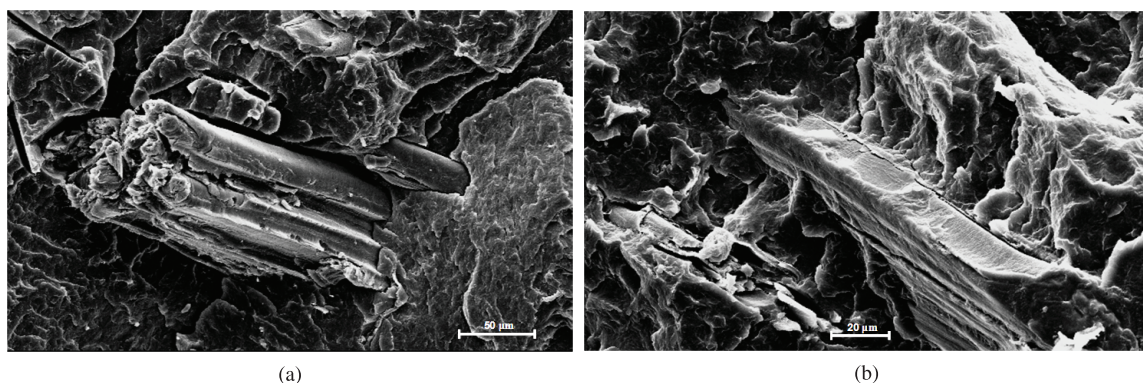


**Figure 7.** Micrographs of polymer/ wood composites: a) without compatibilizer; b) with 10% PP-g-MA.

values were performed, considering  $n$  and  $K$  parameters, and it was found deviations not higher than 4%, proving a good fit for Avrami parameters calculation.

As expected, raising the temperature of isothermal crystallization increases the  $t_{1/2}$ , thus decreasing  $K$  due to the difficulty of crystal nucleation at elevated temperatures. The vPP presented a comparatively longer  $t_{1/2}$  than rPP at all the temperatures applied to crystallize the materials. This corroborates the discussion about Figure 3, i.e., reprocessed PP nucleates more easily than vPP.

The addition of wood flour to both polypropylene (vPP and rPP) kept  $t_{1/2}$  value high. This was attributed to the lack of adhesion between the PP transcrystalline layer and the wood particles, an incompatibility that prevents successful nucleation, where wood acts like a physical barrier. However, the  $t_{1/2}$  was reduced by the use of compatibilizers, particularly the PP-g-AA, and their concentrations did not significantly affect the  $t_{1/2}$ . PP-g-AA is an efficient nucleating agent and the higher its concentration the lower the  $t_{1/2}$ , and hence, the higher the rate of crystallization. In the case of both compatibilizers, this feature is attributed to the effective compatibilization between PP and wood flour, whose blends showed the best interfacial adhesion, according to Figure 7. This figure shows the SEM micrograph for composite with and without compatibilizer. The presence of this component leads to a higher wettability between wood flour particles and PP matrix, which results in better adhesion.

### Crystallization activation energy

The crystallization activation energy can be calculated using the crystallization rate constant ( $K$ ) obtained from the intercept of the Avrami curves. Thus,  $K$  can be described by an Arrhenius relationship, according to Equation 2<sup>[29]</sup>:

$$\frac{1}{K^n} = K_0 \cdot \exp\left(-\frac{E_a}{RT_c}\right) \quad (2)$$

where  $K_0$  is a temperature-independent constant,  $E_a$  is the crystallization activation energy,  $T_c$  is the crystallization temperature, and  $R$  is the gas constant. An  $\ln(K)^{1/n}$  vs.  $1/T_c$  plot gives  $E_a/R$  as the slope and  $\ln K_0$  as the intercept with the y-axis. Figure 8 depicts the results of all the tested compositions.

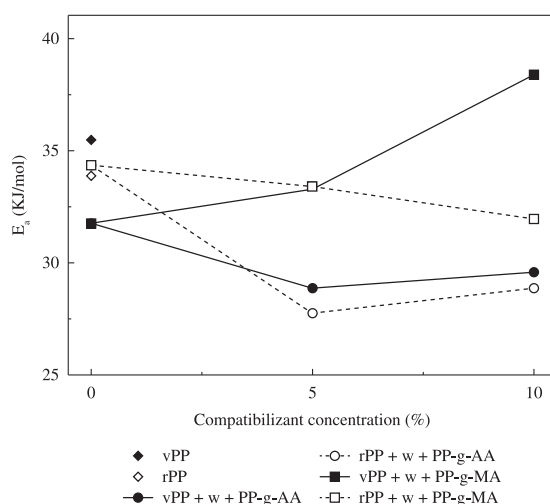


**Figure 8.** Crystallization activation energy ( $E_a$ ) of the compositions.

The addition of PP-g-AA compatibilizer in both vPP and rPP reduced their activation energies, considering also the value of  $E_a$  for pure virgin PP. The presence of this coupling agent favors crystal nucleation, reducing the activation energy needed in this stage. The PP-g-MA compatibilizer had the same effect on the rPP matrix but the opposite effect on vPP, i.e., the crystallization activation energy increased in response to higher concentrations of this compatibilizer. High crystallization activation energy means lower crystallization rates, which hinder the development of the crystallization process. However, Zhao et al.<sup>[32]</sup> stated that this behavior may be the result of the dual effect of compatibilizers, which can work as nuclei for heterogeneous crystallization, facilitating crystal nucleation and growth, particularly at the interface. On the other hand, nucleating agents can hinder the transfer of macromolecules from the polymer melt to the crystal surface growing at the wood-polymer interface due to the weak interaction between compatibilizer and polymer chains, thus increasing the activation energy. In our work, the vPP compositions compatibilized with PP-g-MA showed the latter behavior. However, nucleation is the controlled stage of crystallization and an increase in the nucleation rate leads to a higher total crystallization rate and crystallization temperature.

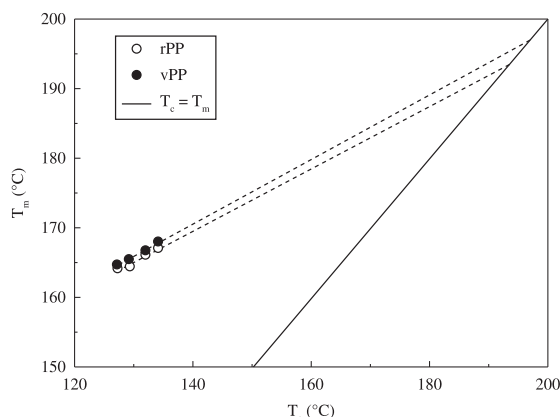


**Figure 9.** Hoffman-Weeks plot for vPP and rPP, both of which show  $r^2 > 0.999$ .

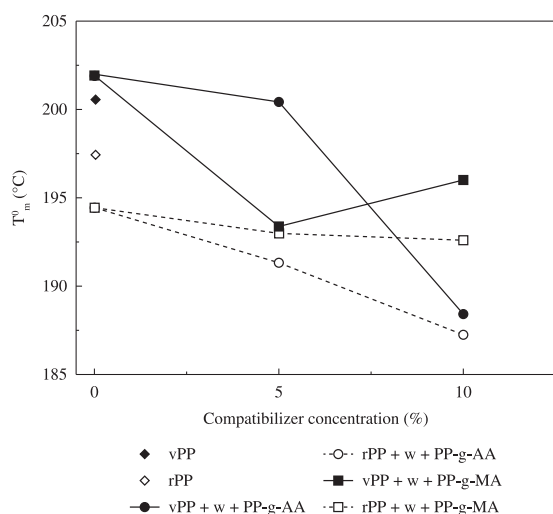


**Figure 10.** Plot of  $T_m^0$  as a function of compatibilizer concentration in vPP and rPP.

### Equilibrium melting temperature

Hoffman-Weeks plots enable the calculation of the equilibrium melting temperature ( $T_m^0$ ), which is the melting temperature of a crystal with a hypothetical infinite lamellar thickness. According to this concept, the thicker a crystal layer the higher its melting temperature. This value is determined by plotting the melting temperature of the resulting crystals vs. the isothermal crystallization temperature ( $T_c$ ), by the intercept of the regression line of the extrapolated data with the equation line  $T_m = T_c$ . Figure 9 illustrates this plot for vPP and rPP. The other samples showed the same behavior, and are therefore not described here. The lowest value of  $r^2$  was 0.985 for vPP with wood flour and 5% PP-g-AA, which shows that all the regressions are statistically reliable.

The polypropylene melting temperature increases as the crystallization temperature of PP crystals increases. A higher  $T_c$  gives rise to a higher  $T_m$  because higher temperatures favor growth mechanisms, resulting in thicker crystals. Figure 10 depicts the  $T_m^0$  values of vPP and rPP and their wood composites as a function of compatibilizer concentration.

Pure vPP has greater  $T_m^0$  than rPP. A similar behavior was observed by Rabello and White<sup>[27]</sup> for photodegraded polypropylene and was attributed to decrease in molecular weight and increase on crystallites imperfection due to degradative process. However, the addition of wood flour to both polypropylene blends inverted this behavior. All the compositions containing rPP showed lower values of  $T_m^0$ . The general tendency was for the addition of compatibilizer to reduce the  $T_m^0$ . Wood flour particles can lead to the formation of unstable and imperfect spherulites. Lopez-Machado and Arroyo<sup>[33]</sup> reached the same conclusion for polypropylene/ synthetic fibers.

The bonds formed between polymer composites and wood favor the nucleation of small crystals. In fact, increasing the concentration of compatibilizer improved the adhesion between wood and polymer, and also reduced the  $T_m^0$  value. This finding was confirmed by the crystallization activation energy data, whose lower values in the samples containing compatibilizer were attributed to their nucleating effect on polypropylene.

### Conclusions

The rheological tests indicated that the reprocessed polypropylene underwent degradation by chain scission and narrowing of the MWD. The Avrami plots indicated that rPP became completely crystallized in less time than vPP at all the isothermal crystallization temperatures. Non isothermal results showed that rPP nucleates faster than vPP and reinforced the nucleating effect of wood. The value of  $n$  remained between 1.9 to 2.3, indicating crystals with two dimensions and instantaneous nucleation, and this parameters was not influenced by reprocessing, presence of wood and compatibilization. The crystallization half-time of rPP is lower than vPP and decreased with both compatibilizers, particularly with PP-g-AA, due to enhanced adhesion at the wood-polypropylene interface, as observed in SEM micrographs. The vPP-wood composites without compatibilizer showed the highest values of crystallization half-time. The crystallization activation energy was lower for the rPP matrix and PP-g-AA compatibilizer. The equilibrium melting temperature was higher for vPP than rPP and the increase in compatibilizers concentration decreased  $T_m^0$  values.

### Acknowledgements

The authors acknowledge the Brazilian research funding agencies CAPES, CNPq and Fundação Araucária for their financial support of this work. We are also indebted to the companies Braskem, Chemtura and Pinhopó for their donation of polypropylene, compatibilizers, and wood flour, respectively.

### References

- Correa, C. A.; Fonseca, C. N. P. & Neves, S. - *Polímeros*, **13**, p.154, (2003). <http://dx.doi.org/10.1590/S0104-14282003000300005>
- Zhang, Y.; Togiani, H.; Zhang, J.; Xue, Y. & Pittman, C. U. - *J. Mater. Sci.*, **44**, p.2143 (2009). <http://dx.doi.org/10.1007/s10853-009-3295-0>



3. Borysiak, S. – Polym. Bull., **64**, p.275 (2010). <http://dx.doi.org/10.1007/s00289-009-0202-4>
4. Dányádi, L.; Janecska, T.; Szabó, Z.; Nagy, G.; Móczó, J. & Pukánsky B. – J. Comp. Sci. Tech., **67**, p.2838 (2007). <http://dx.doi.org/10.1016/j.compscitech.2007.01.024>
5. Lisperguer, J.; Droguett, C.; Ruf, B. & Nuñez, M. – J. Chil. Chem. Soc., **52**, p.1073 (2007).
6. Ashori, A. & Nourbakhsh, A. – J. Bior. Tech., **101**, p.2515 (2010). PMID:19948401. <http://dx.doi.org/10.1016/j.biortech.2009.11.022>
7. Vianna, W. L.; Correa, C. A. & Razzino, C. A. - Polímeros, **14**, p.339 (2004).
8. Pinheiro, L. A.; Chinelatto, M. A. & Canevarolo, S. V. – Polym. Degrad. Stab., **86**, p.445 (2004). <http://dx.doi.org/10.1016/j.polyimdegradstab.2004.05.016>
9. Pinheiro, L. A.; Hu, G.-H.; Pessan, L. A. & Canevarolo, S. V. – Polym. Eng. Sci., **48**, p.806 (2008). <http://dx.doi.org/10.1002/pen.21009>
10. Pinheiro, L. A.; Bitencourt, C. S. & Canevarolo, S. V. – Polym. Eng. Sci., **50**, p.826 (2010). <http://dx.doi.org/10.1002/pen.21594>
11. Melo, T. J. A.; Pinheiro, L. A. & Canevarolo, S. V. – Polímeros, **20**, p.322 (2010). <http://dx.doi.org/10.1590/S0104-14282010005000050>
12. Nunez, A. J.; Sturm, P. C.; Kenny, J. M.; Aranguren, M. I.; Marcovich, N. E. & Reboredo, M. M. – J. Appl. Polym. Sci., **88**, p.1420 (2003). <http://dx.doi.org/10.1002/app.11738>
13. Paul, S. A.; Oommen, C.; Joseph, K. & Mathew, G. – Polym. Comp., **31**, p.1113 (2010).
14. Harper, D. & Wolcott, M. – Compos. part A: Appl Sci Manuf., **35**, p.385 (2004). <http://dx.doi.org/10.1016/j.compositesa.2003.09.018>
15. Carvalho, B. M.; Bretas, R. E. S. & Isayev, A. I. – J. Appl. Polym. Sci., **73**, p.2003 (1999). [http://dx.doi.org/10.1002/\(SICI\)1097-4628\(19990906\)73:10<2003::AID-APP19>3.0.CO;2-J](http://dx.doi.org/10.1002/(SICI)1097-4628(19990906)73:10<2003::AID-APP19>3.0.CO;2-J)
16. Carvalho, B. M. & Bretas, R. E. S. – J. Appl. Polym. Sci., **68**, p.1159 (1998). [http://dx.doi.org/10.1002/\(SICI\)1097-4628\(19980516\)68:7<1159::AID-APP13>3.0.CO;2-T](http://dx.doi.org/10.1002/(SICI)1097-4628(19980516)68:7<1159::AID-APP13>3.0.CO;2-T)
17. Carvalho, B. M. & Bretas, R. E. S. – J. Appl. Polym. Sci., **72**, p.1741 (1999). [http://dx.doi.org/10.1002/\(SICI\)1097-4628\(19990624\)72:13<1741::AID-APP10>3.0.CO;2-0](http://dx.doi.org/10.1002/(SICI)1097-4628(19990624)72:13<1741::AID-APP10>3.0.CO;2-0)
18. Kim, J.-W.; Harper, D. P. & Taylor, A. M. – J. Appl. Polym. Sci., **112**, p.1378 (2009). <http://dx.doi.org/10.1002/app.29522>
19. Causin, V.; Marega, C.; Saini, R.; Marigo, A. & Ferrara, G. – J. Thermal. Anal. Calor., **90**, p.849 (2007). <http://dx.doi.org/10.1007/s10973-006-8205-y>
20. Wei, Z. Y.; Zhang, W. X.; Chen, G. Y.; Liang, J. C.; Chang, Y.; Liu, L. A.; Wang, P. & Sun, J. C. – J. Thermal. Anal. Calor., **103**, p.701 (2011). <http://dx.doi.org/10.1007/s10973-010-0958-7>
21. Nath, D. C. D.; Bandyopadhyay, S.; Yu, A. B.; Blackburn, D.; White, C. & Varughese, S. – J. Thermal. Anal. Calor., **99**, p.423 (2010). <http://dx.doi.org/10.1007/s10973-009-0408-6>
22. Sclavons, M.; Franquinet, P.; Carlier, V.; Verfaillie, G.; Fallais, I.; Legras, R.; Laurent, M. & Thyron, F. C. – Polymer, **41**, p.1989 (2000). [http://dx.doi.org/10.1016/S0032-3861\(99\)00377-8](http://dx.doi.org/10.1016/S0032-3861(99)00377-8)
23. D'Avila, M. A. & Bretas, R. E. S. - “Reologia de polímeros fundidos”, 2. ed, Edufscar, São Carlos (2005).
24. Canevarolo, S. V. – Polym. Degr. Stab., **70**, p.71 (2000). [http://dx.doi.org/10.1016/S0141-3910\(00\)00090-2](http://dx.doi.org/10.1016/S0141-3910(00)00090-2)
25. Babetto, A. C. & Canevarolo, S. V. – Polímeros, **10**, p.90 (2000). <http://dx.doi.org/10.1590/S0104-14282000000200011>
26. Caceres, C. A. & Canevarolo, S. V. – Polímeros, **16**, p.294 (2006). <http://dx.doi.org/10.1590/S0104-14282006000400008>
27. Rabello, M. S. & White, J. R. – Polymer, **38**, p.6389 (1997). [http://dx.doi.org/10.1016/S0032-3861\(97\)00214-0](http://dx.doi.org/10.1016/S0032-3861(97)00214-0)
28. Somnuk, U.; Eder, G.; Phinyocheep, P.; Suppakarn, N.; Sutapun, W. & Ruksakulpiwat, Y. – J. Appl. Polym. Sci., **106**, p.2997 (2007). <http://dx.doi.org/10.1002/app.26883>
29. Zhang, C.-F.; Bai, Y.-X.; Gu, J. & Sun, Y.-P. – J. Appl. Polym. Sci., **122**, p.2442 (2011). <http://dx.doi.org/10.1002/app.34429>
30. Jonas, A. & Legras, R. – Polymer, **32**, p.2691 (1991). [http://dx.doi.org/10.1016/0032-3861\(91\)90095-Z](http://dx.doi.org/10.1016/0032-3861(91)90095-Z)
31. Quillin, D. T.; Yin, M. P.; Koutsky, J. A. & Caulfield, D. F. – J. Appl. Polym. Sci., **52**, p.605 (1994). <http://dx.doi.org/10.1002/app.1994.070520504>
32. Zhao, G. D.; Pan, Z. L.; Wang, J.; Guo Q. & Cai, X. F. – J. Macromol. Sci. part B: Phys. **50**, p.821 (2011).
33. Lopez-Machado, M. A. & Arroyo, M. – Polymer, **40**, p.487 (1999). [http://dx.doi.org/10.1016/S0032-3861\(98\)00198-0](http://dx.doi.org/10.1016/S0032-3861(98)00198-0)

Received: 27/05/12

Revised: 22/08/12

Accepted: 01/11/12